Journal of Environmental Science Studies; Vol. 6, No. 2, 2023
ISSN 2591-779X E-ISSN 2630-4821
Published by July Press

Experimental Investigation on Countermeasures for Gravel Bed Scouring and Driftwood Deposition Around Pier

Youichi Yasuda[1] & Toshiki Ishitsuka[2]

[1] Department of Civil Engineering, College of Science and Technology, Nihon University, Tokyo, Japan

[2] Department of Civil Engineering, Graduate School of Science and Technology, Nihon University, Tokyo, Japan

Correspondence: Prof. Youichi Yasuda, Civil Engineering Dept., College of Sci. and Tech., Nihon University, Tower Schola S1010, 1-8-14 Kanda Surugadai, Chiyoda-ku, 101-8308 Tokyo, Japan. E-mail: yasuda.youichi@nihon-u.ac.jp

Received: August 12, 2023 Accepted: September 13, 2023 Online Published: December 13, 2023

doi:10.20849/jess.v6i2.1395 URL: https://doi.org/10.20849/jess.v6i2.1395

Abstract

During floods, driftwood is generated simultaneously with sediment runoff, may impinge and accumulate on bridge piers. In this case, the water level rises upstream of the bridge, flooding from the river, resulting in major damage, such as overtopping and collapse of houses and bridges. Further, a high velocity flow passing over the pier due to impact of the flow at the upstream face of the pier causes scouring of the river bottom around the pier. In this study, the installation of consecutively assembled boulders was proposed in order to protect against scouring around the pier. A trapezoidal elliptical shape pier was also proposed as a countermeasure to reduce driftwoods capturing. As a comparative study, revetment blocks, which are conventionally used as countermeasure works, were installed. The experimental results revealed that the proposed structure was effective in reducing driftwood deposition and preventing gravel bed scouring, based on analysis using flow velocity with time series variation, vector diagrams, and driftwood model.

Keywords: pier shape, flood flow, local scouring, consecutively assembled boulders, driftwood

1. Introduction

The piers supporting river-crossing bridges are subjected to the problem of driftwood and other debris that may be deposited in front of the piers during a flood event during flood stages. The accumulation of driftwood and other debris on the bridge piers can lead to rising water levels and severe flooding. In this case, the water level rises upstream of the bridge, causing the river to overflow, resulting in extensive damage such as the loss or collapse of homes, bridges, and other structures. In addition, a three dimensional flow formed by the impact of the approaching flow on the upstream face of the bridge piers creates a deflected flow toward the riverbed, causing damage that transports riverbed gravels. A local scour around the piers occurs, and the gravel layer supporting the bottom of the piers is eroded, resulting in the piers' deflection and collapse. In accordance with the shape of piers, the structure should not significantly impede the flow during floods, and the flat shape may be an elongated oval or similar shape as much as possible in order to reduce the rate of river blockage (Japan River Association., 2005).

The flow characteristics around piers and scouring of riverbeds was studied, including the flow around columns and scouring of riverbeds due to different column diameters (Ettema et al., 2006), and scouring of riverbeds due to exposure of the base of piers (Umeda et al., 2010). There are also studies the riverbed scouring due to different pier geometries (Vijayasree et al., 2019). Regarding driftwood deposition, hydrodynamic forces acting on bridges were investigated when driftwood is deposited on piers (Maeno et al., 2014, Watanabe et al., 2015). The effects of streambank erosion caused by diverted flow (Okamoto et al., 2017) and the effect of driftwood deposition on the length and thickness of driftwood was also been studied (Furlar et al., 2018).

In general, mechanisms of riverbed scour around piers have been studied, but there are few examples and studies of countermeasures, leaving room for further investigation. Although riprap has been considered as a measure to prevent riverbed scouring around piers. Riprap layers installed to prevent riverbed scour can cause complete collapse failure or embedded failure (Chiew et al., 2002 and 2005). Zhang (2022) described that riprap increases the strength of the riverbed near the foundation by replacing the soil near the bridge pier with heavier and larger stones, thereby strengthening the bearing capacity of the riverbed near the foundation to the vortex and reducing the maximum scour depth. He also pointed that there are four common failure types in riprap: shear failure, destabilized failure, edge failure and winnowing failure, among which winnowing failure has the most significant impact on the stability of riprap (2022). Others have shown that the combination of collars and riprap as a measure to prevent riverbed scour can reduce the extent of riprap placement and the quantity of riprap stones (Zarrati et al., 2004). Other measures to prevent scour around piers are proposed, such as the installation of bagged rock removal methods (Inoue et al., 2021).

Recently, Yasuda and Fuchino (2022) showed the installation of consecutively assembled boulders might be effective as a balance between stabilization of structure during flood stages and environmental improvement.

In the field, there is no established method of protecting the downstream riverbed of piers installed in rivers with large bedrock, resulting in riverbank erosion and scour. Further, the shape of the piers in order that driftwood does not accumulate in front of the piers has not been clarified.

The authors investigated the effect of installing consecutively assembled boulders on riverbed scour around the pier. The installation of the consecutively assembled boulders was compared with that of the conventional revetment blocks. The physical model with 1/10 scale was applied on the basis of Froude similarity. In this experiment, the aspect ratio of the width of the water flow on both sides of the piers to the depth of the flow was set to be small in order to consider the safe side of the revetment around the piers due to the three-dimensional flow passing through the piers. Furthermore, a trapezoidal elliptical shape pier shape with a tilted pier front was proposed as a countermeasure to reduce driftwood trapping, and an experimental study was conducted including a comparison with a long rectangle elliptical shape pier. The effects on the riverbed were studied by examining the time-series changes in the time-averaged flow velocity and flow velocity in the protected section and downstream of the protected section during a flood event, and the differences in driftwood trapping reduction by pier shape were examined using a driftwood model.

2. Experimental Set-up

A rectangular cross-section horizontal channel (channel width B = 0.80 m, length 17 m, height 0.60 m) was used for the experiment. The symbol definition diagram is shown in Figure 1. Two different types of piers were placed around the piers to investigate scouring of the gravel bed around the pier. At the center of the channel, a 0.475 m high, d = 0.10 m diameter, 0.45 m long in the downstream direction (Figure 2 (a)) or a 0.90 m long trapezoidal elliptical shape model (Figure 2 (b)). In the trapezoidal elliptical shape was installed in front of the 0.45 m long rectangle elliptical shape model with a d = 0.10 m diameter in the downstream direction, which was integrated with a triangular member (the space was reinforced with wood) made of 1-mm-thick PVC plates at a 45-degree angle of inclination. Further, the installation of consecutively assembled boulders with that of the bed-protection blocks was compared. The protection blocks were hollow-scare type blocks with 0.10 m long, 0.10 m wide, and 0.03 m height as shown in Figure 3 (a). The consecutively assembled boulders were crushed stones with averaged size 0.07 m in which was averaged long length, short length, and height. In addition, gravels with 0.002 to 0.015 m sizes (Figure 3 (b)) were placed in the upstream and downstream area of the protection area to investigate the scouring of the riverbed. To adjust the positive step at the upstream end (0.021 m step between the channel bottom and the movable bed), a steel plate was installed upstream at a 1/25 gradient. To investigate the possibility of driftwoods trapping in front of pier under different shapes of piers, a 0.0015m mesh net (0.60 m long, 0.10 m wide, and 0.10 m high) with several pieces of wood and wire mesh entangled in it, as shown in Figure 3 (c), was used to simulate driftwood that could be separated.

The experimental conditions are shown in Table 1. In Case 1, the pier is a long rectangle elliptical shape pier, and conventional protection blocks were installed on both sides of the pier. In Case 2, the pier is the long rectangle elliptical shape pier, and the consecutively assembled boulders are installed on both sides of the pier as a protection region. In Case 3, the pier is the long rectangle elliptical shape pier, and the consecutively assembled boulders are installed in 1.8 times region of Case 2. In Case 4, the pier is a trapezoidal elliptical shape pier, and the consecutively assembled boulders are installed on both sides of the pier.

Water depth and gravel bed profiles were measured using a point gauge (legible to 1/10 mm). The transported gravels downstream of the test region were collected after 15 or 30 hours. Velocity measurements were made using two-dimensional electromagnetic anemometers with type I probe (capable of measuring the downstream and lateral components) and type L probe (capable of measuring the downstream and vertical components) (sampling time: 90 sec, sampling frequency: 0.05 sec (20 Hz)). As shown in Figure 1, the depth and bed profiles were recorded using the following three axes: the x-axis for the downstream direction with the upstream end of the pier as the origin; the y-axis for the cross-sectional direction with the center of the channel as the origin and the left bank as the positive direction; and the z-axis for the vertical upward direction with the riverbed before the experiment as the origin. The plan velocities measurement was conducted at four cross-sections of y = 0.00 m ((2y-Bp)/(B-Bp) = 0.00) (center of channel), y = 0.09 m ((2y-Bp)/(B-Bp) = 0.11) (near the pier), y = 0.17 m ((2y-Bp)/(B-Bp) = 0.34) (center of the left bank side), and y = 0.32 m ((2y-Bp)/(B-Bp) = 0.77) (sidewall side). The effect of front shape of pier on accumulation of driftwood was examined by transporting several driftwood models in the channel from the upstream side, and recording the condition in which the driftwood was caught in front of the bridge piers.

Table 1. Experimental conditions

Case	Q(m^3/s)	h_d(m)	L_a/B	L_b/B	L_c/B	L_p/B	B_p/B
1	0.144	0.247	0.500	0.625	0.875	0.563	0.125
2		0.249					
3		0.249		1.125			
4		0.247				1.125	

Note: Q = discharge, h_d = downstream water depth

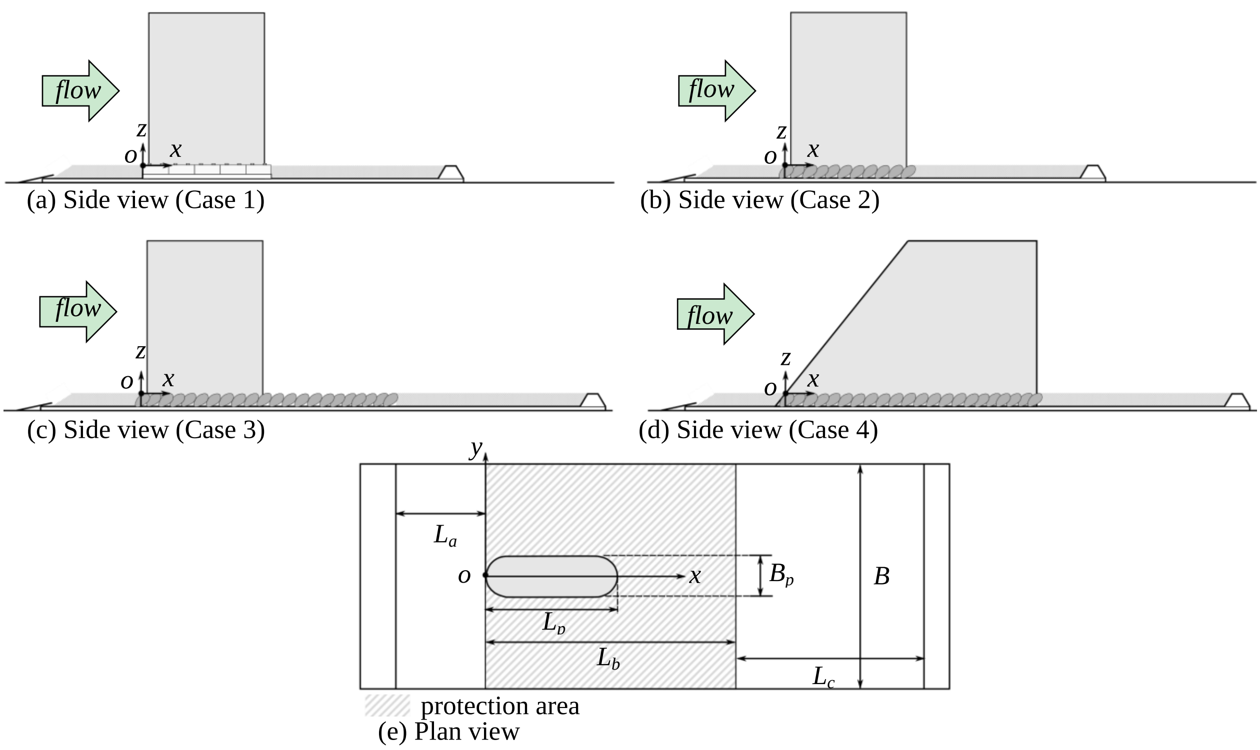

Figure 1. Symbol definition diagram

(a) Long rectangle elliptical shape pier (b) Trapezoidal elliptical shape pier

Figure 2. Physical models of Pier

(a) Boulders and Protection blocks (b) Gravels (c) Driftwood models

Figure 3. Boulders and protection blocks, and gravels, and driftwood models

3. Results

3.1 Scour Downstream of Piers

Figure 4 shows the gravel surface profiles downstream of the protection region after more 15 hours in experimental period for each case (Cases 1, 2, 3, and 4).

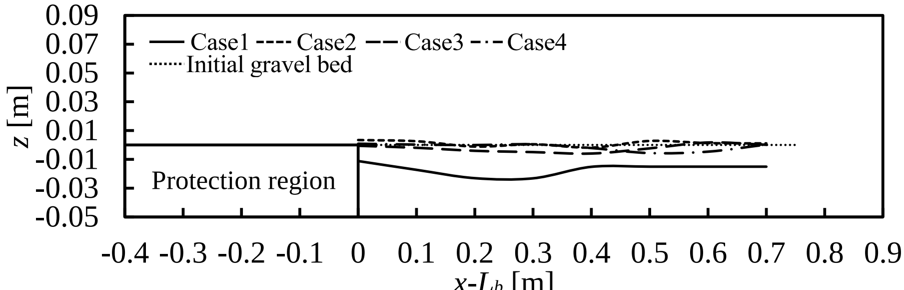

(a) y = 0.09 m ((2y-Bp)/(B-Bp) = 0.11)

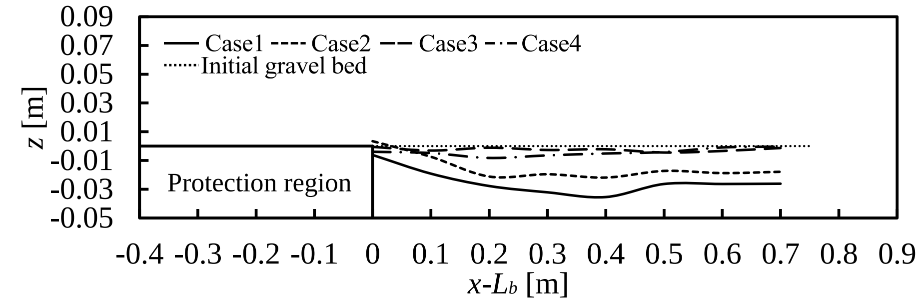

(b) y = 0.17 m ((2y-Bp)/(B-Bp) = 0.34)

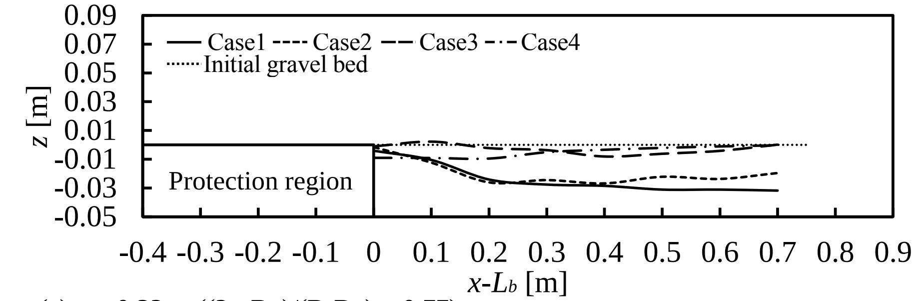

(c) y = 0.32 m ((2y-Bp)/(B-Bp) = 0.77)

Figure 4. Gravel surface profiles downstream of the protection region

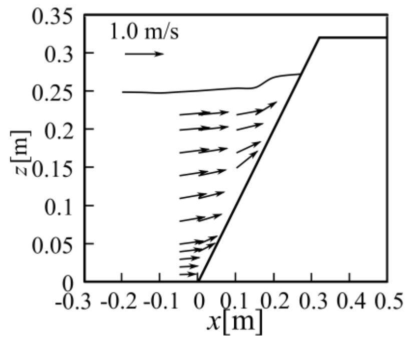

Figure 5. The velocity vectors upstream of the trapezoidal elliptical shape pier. (y = 0 m, smooth bed, h_d = 0.24 m)

As shown in this figure, in Case 1, a typical local scouring was formed downstream of the protection block, and scour depth is always larger than that for Cases 2, 3, 4. In Case 2, the consecutively assembled boulders were within the long rectangle elliptical shape pier (see Figure 1 (b)), and small local scouring was formed except for center part of channel. The scouring may be caused by the formation of a three-dimensional flow passing through the assembled boulders. Comparison between Case 1 and Case 2 yields that the velocity decay near the consecutively assembled boulders may reduce scouring downstream of the protection region. In Case 3, by considering the formation of a three dimensional flow due to the impingement of pier, the installation region of assembled boulders was expanded to 1.8 times larger than that for Case 2, and there was no scouring downstream of the protection area after 30 hours in the experimental period. In Case 4, the assembled boulders were installed within the region of trapezoidal elliptical shape pier (see Figure 1 (d)), as shown in Figure 4, scouring is limited after 30 hours of experimental period. Furthermore, as the impingement location changes with the vertical direction, as shown in Figure 5, an upward flow is always observed along the upstream face of pier, and there is no scouring of the gravel bed immediately upstream of the pier. On the other hand, in the case of the long rectangle elliptical shape pier, a small scouring was observed at the front of the pier. In this case, as the upstream surface of the pier is a vertical surface, scouring may be caused by the formation of horseshoe vortex due to a downward flow.

3.2 Effects of Driftwood Capture Mitigation Measures

Figure 6 shows the possibility of driftwood depositions in Case 3 and 4, as seen from the upstream and sidewalls of the pier, when the driftwood model shown in Figure 3 (c) was transported from the upstream side.

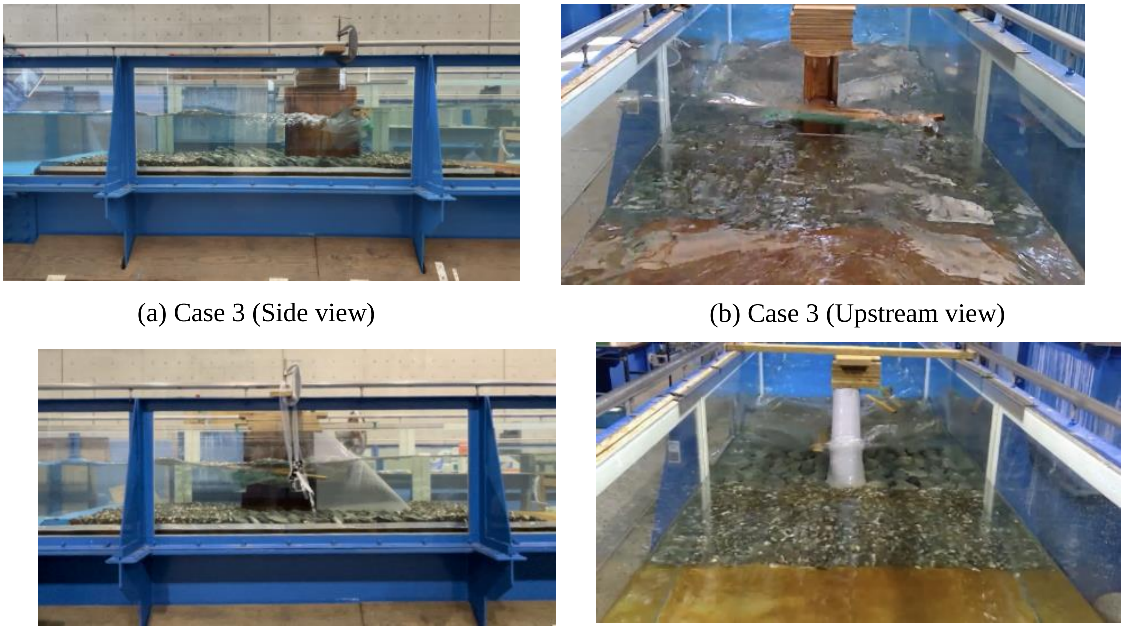

(a) Case 3 (Side view) (b) Case 3 (Upstream view)

(c) Case 4 (Side view) (d) Case 4 (Upstream view)

Figure 6. Possibility of driftwood depositions under different types of pier shapes

In the case of Case 3 (Figure 6 (a) and (b)), where the pier shape is a long rectangle elliptical, driftwood accumulation was observed on the front side of the pier. It might be caused that the front of the long rectangle elliptical shape is vertical, and the impingement position on the front of the pier does not change with the vertical direction, and driftwood tends to deposit at the front of the pier at the same time as the impact. On the other hand, in the case of trapezoidal elliptical shape pier Case 4 (Figure 6 (c), (d)), driftwood was not deposited in front of the pier but was washed downstream. In the case of the trapezoidal elliptical shape pier, the front of the pier is tilted, which tends to disperse the impact on the front of the pier, causing instability of the driftwood, which tends to flow out without depositing on the front of the pier.

The water level upstream of the pier is higher for the long rectangle elliptical shape than for the trapezoidal elliptical shape. In the case of the long rectangle elliptical shape, the water level upstream of the pier tends to rise further due to driftwood accumulation in front of the pier. This indicates that the trapezoidal elliptical shape can reduce deposition of driftwoods and thereby may reduce increasing water level upstream of the pier.

3.3 Water Surface and Bed Profiles and Time-averaged Velocity Profiles Around the Piers

Figure 7 shows the water surface and bed profiles and time-averaged velocity distribution of $\bar{u}$ in the downstream component (x-direction) around the piers in each case. The left side figure shows these profiles near the pier ($y = 0.09$ m ($(2y-Bp)/(B-Bp) = 0.11$)) and the right side figure shows those near the sidewall ($y = 0.32$ m ($(2y-Bp)/(B-Bp) = 0.77$)). The red circles in Figure 7 indicate the locations just below the assembled boulders (detail discussion in Chapter 6).

Regarding the water surface profiles around the pier, when the pier shape is a long rectangle elliptical shape pier, the effect of the weir uplift due to the impact on the front of the pier is larger than that of a trapezoidal elliptical shape pier, and the water surface irregularity on the sidewall side is larger due to the flow impact on the front of the pier (Figure 7 (b), (d) and (f)). On the other hand, when the pier shape is trapezoidal elliptical, the water surface irregularity on the sidewall side is smaller than that of the long rectangle elliptical shape because the impact position on the pier front is different in the water depth direction (Figure 7 (h)). Therefore, the trapezoidal elliptical shape pier results in smaller water surface irregularity on the sidewall side.

The time-averaged velocity of the x-component near the pier (y = 0.09 m ((2y-Bp)/(B-Bp) = 0.11) shows that in Case 1 (Figure 7 (a)), the velocity accelerates in the area where the water surface becomes convex downward due to the impact on the front of the pier. In addition, the main current is located near the riverbed at the upstream side of the protection works section, and its influence extends downstream. On the other hand, in Case 2 (Figure 7 (c)), where consecutively assembled boulders are placed on both sides of the piers, the flow velocity accelerates upstream of the protection works section as in Case 1, but the flow velocity near the bottom attenuates as it moves downstream, and the mainstream tends to rise toward the water surface. In Cases 3 and 4 (Figure 7 (e) and (g)), the protected sections are longer than Case 2, so the attenuation of the flow velocity near the bottom is greater.

For the time-averaged velocity of the x-component near the sidewall side (y = 0.32 m ((2y-Bp)/(B-Bp) = 0.77)), Case 1, where protective blocks are installed on both sides of the pier, has a larger velocity gradient not only upstream but also downstream of the protection area (Figure 7 (b)). In Case 2, where the assembled boulders are installed on both sides of the piers (Figure 7 (d)), the water surface becomes uneven at the downstream end of the protection area, resulting in a larger velocity gradient downstream of the protection area, as in Case 1. On the other hand, in Cases 3 and 4 (Figure 7 (f) and (h)), the velocity decay near the bottom is small upstream of the protection area, but the velocity decay near the bottom increases as one moves downstream of the protection area.

Figure 8 shows plan velocity vector with the time-averaged velocity $\bar{u}$ in downward component (x-direction) and $\bar{v}$ in the transverse component (y-direction) at different vertical heights (z-direction) z = 0.05 m, z = 0.11 m, and z= 0.17 m for Cases 3 and 4. The origin of z is defined on the basis of the initial gravel surface. In Case 3, as shown in Figure 8 (a), (c), and (e), the difference of the plane velocity vector in vertical direction is small. In the case of trapezoidal elliptical shape pier (Case 4), as shown in Figure 8 (b), (d), and (f), the plane vectors around the piers are different in the vertical direction because the impingement position of approaching flow is different in the vertical direction. Considering the possibility of driftwood deposition and the difference in plane velocity vectors between the rectangular and trapezoidal elliptical shapes, the driftwood may be momentarily affected by the deflected flow impinging on the upstream face of the trapezoidal elliptical shape, and the instability of the driftwood may suppress driftwood deposition.

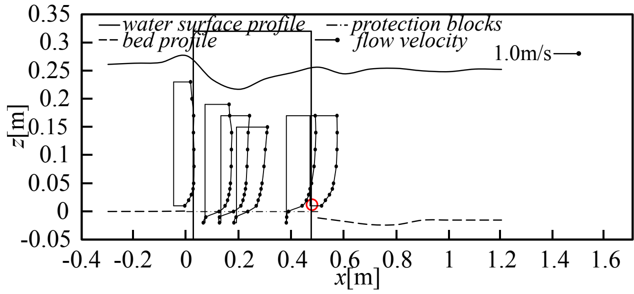

(a) Case 1 (y = 0.09 m ((2y-B_p)/(B-B_p) =

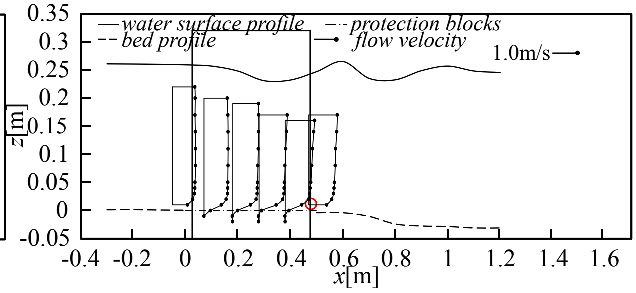

(b) Case 1 (y = 0.32 m ((2y-B_p)/(B-B_p) = 0.77))

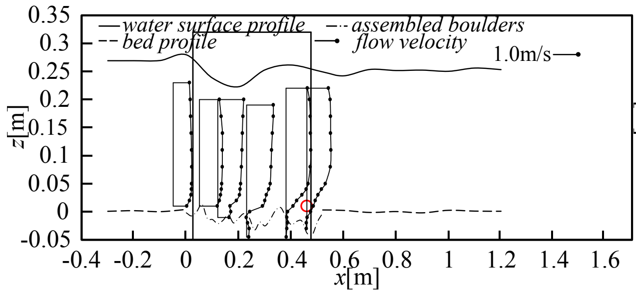

(c) Case 2 (y = 0.09 m ((2y-B_p)/(B-B_p) =

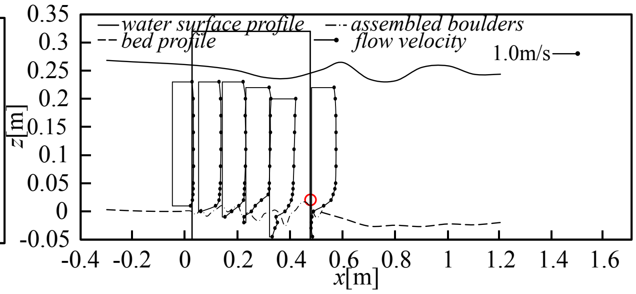

(d) Case 2 (y = 0.32 m ((2y-B_p)/(B-B_p) = 0.77))

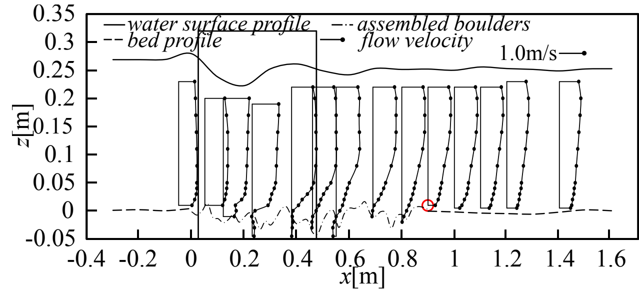

(e) Case 3 (y = 0.09 m ((2y-B_p)/(B-B_p) =

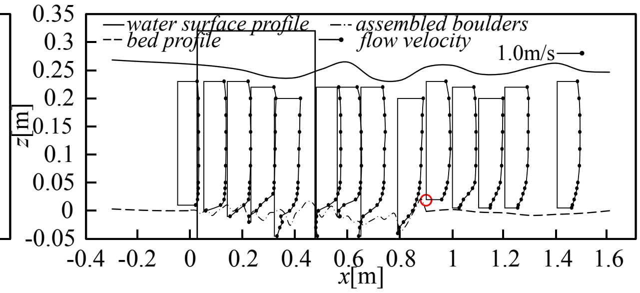

(f) Case 3 (y = 0.32 m ((2y-B_p)/(B-B_p) =

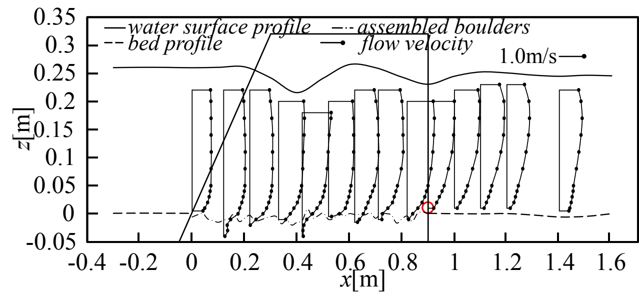

(g) Case 4 (y = 0.09 m ((2y-B_p)/(B-B_p) =

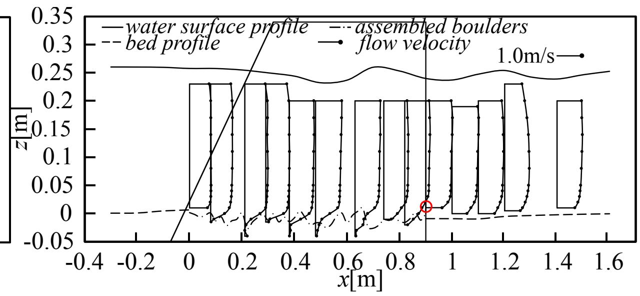

(h) Case 4 (y = 0.32 m ((2y-B_p)/(B-B_p) =

Figure 7. Water surface and gravel bed profiles, and velocity distributions

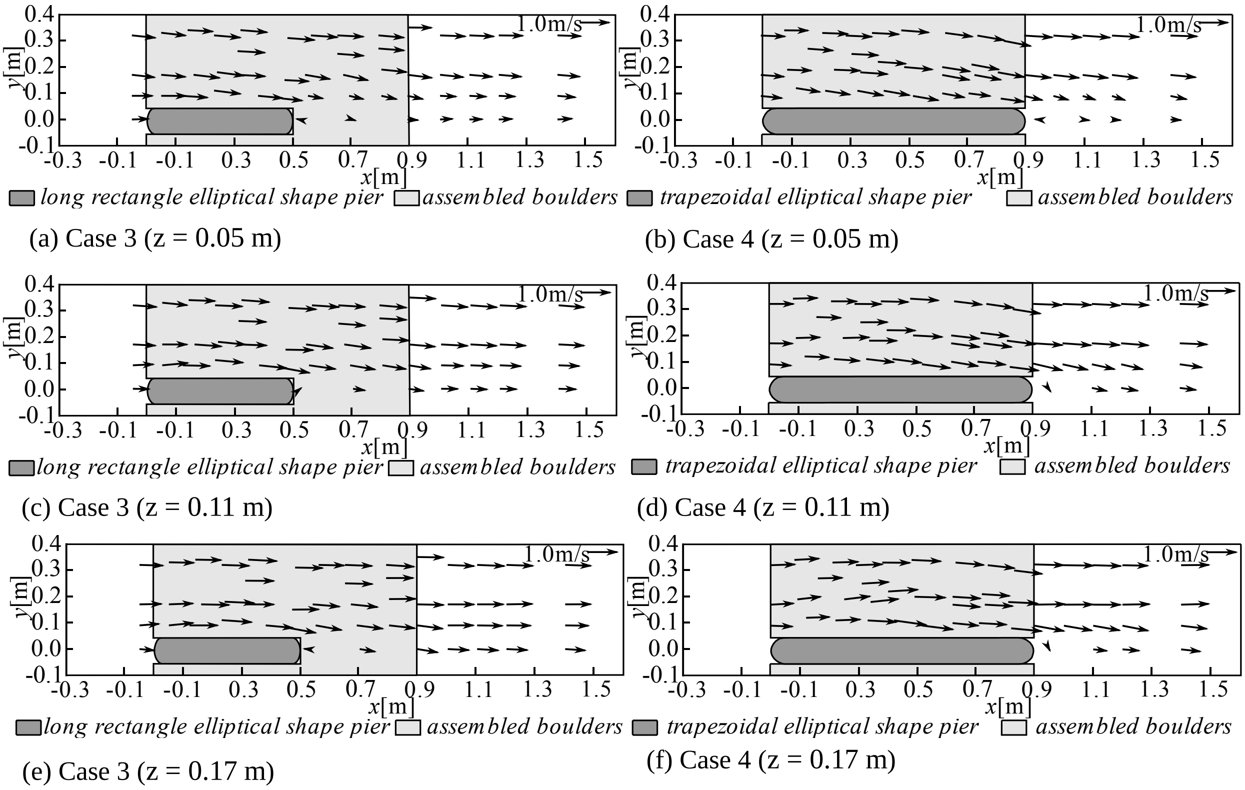

Figure 8. Plane velocity vectors of the time-averaged velocity

3.4 Time-series Variation of Flow Velocity

Figure 9 shows the time-series variation of the flow velocity u in the x-direction near the pier and the sidewall at the downstream end of the protection works in each case during the measurement time (90 seconds). The points indicated by the red circles in Figure 7 are the target points.

In the case of the long rectangle elliptical shape pier, comparing the case of protection blocks (Case 1) (Figure 9 (a) and (b)) with the case of consecutively assembled boulders (Case 2) (Figure 9 (c) and (d)), the time-averaged velocity near the pier for Case 2 (Figure 9 (c)) was smaller than that for Case 1 (Figure 9 (a)) and also the fluctuation range of the velocity for Case 2 was smaller. On the other hand, the time averaged velocity and velocity fluctuation near the sidewall (Figure 9 (b) and (d)), the difference between Case 1 and Case 2 is small. For Case 3, the velocity fluctuation near the pier is somewhat larger than that for Case 2 (Figure 9 (c) and (e)). This might be caused by a flow interference from side walls. Comparing the time averaged velocity near the side wall, the velocity for Case 3 is smaller than that for Case 2 (Figure 9 (d) and (f)). Regarding the fluctuation velocity near the sidewall, similar tendency as in the case near the pier was recorded.

When the pier is trapezoidal elliptical shape pier, the fluctuation range and magnitude of time-averaged velocity near the pier are smaller than those for Case 3 (Figure 9 (e) and (g)). The difference in the width of velocity fluctuation and the magnitude of the time-averaged velocity between Cases 3 and 4 is small near the sidewall (Figure 9 (f) and (h)).

In the case of the long rectangle elliptical shape pier, the impact on the front of the pier cannot be reduced near the sidewall of the downstream end of the pier due to the effect of the unevenness of the water surface (see Figure 7), and the velocity near the gravel bed cannot be reduced compared to the area near the pier. Therefore, it is important to set up the installation of consecutively assembled boulders in the area affected by the flow impinging on the front of the piers. When the pier shape is trapezoidal elliptical shape, the influence of the flow impinging on the pier front can be reduced by installing the assembled boulders on both sides of the pier.

The time-series variation of the flow velocity u in the downstream direction is described here, but the time-series variation of the flow velocity v in the transverse direction has a smaller variation range than that of the flow velocity in the downstream direction. Therefore, the effect of transverse velocity on transport of gravels is considered to be smaller than that of the velocity in the downstream direction. In addition, the difference in the transverse component of the flow velocity due to the different shapes of the piers is small.

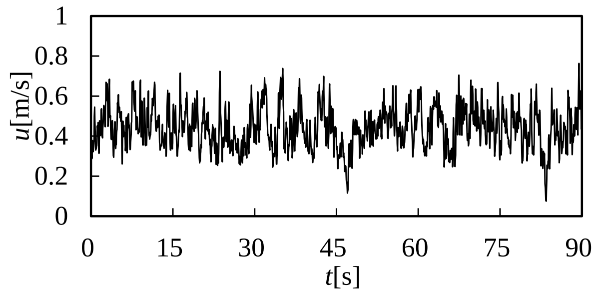

(a) Case 1 (x = 0.47 m, z = 0.01 m, y = 0.09 m ((2y-B_p)/(B-B_p) = 0.11))

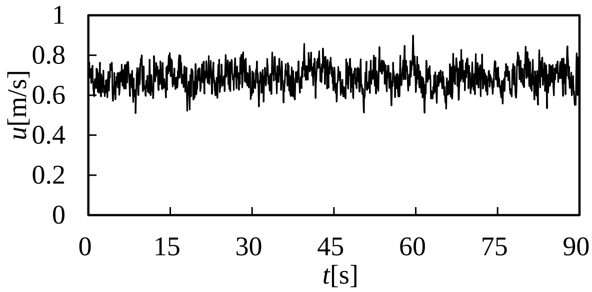

(b) Case 1 (x = 0.47 m, z = 0.01 m, y = 0.32 m ((2y-B_p)/(B-B_p) = 0.77))

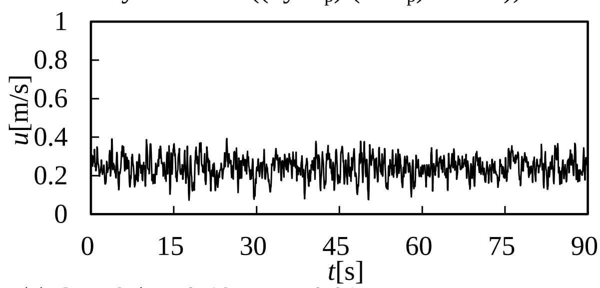

(c) Case 2 (x = 0.46 m, z = 0.01 m, y = 0.08 m ((2y-B_p)/(B-B_p) = 0.09))

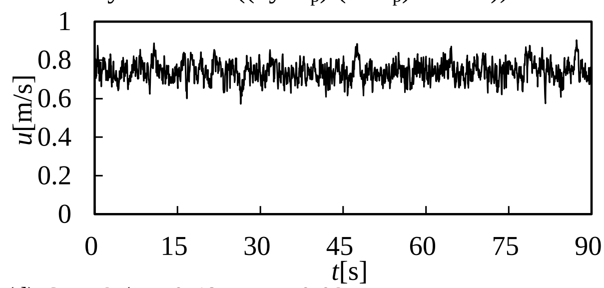

(d) Case 2 (x = 0.48 m, z = 0.02 m, y = 0.32 m ((2y-B_p)/(B-B_p)= 0.74))

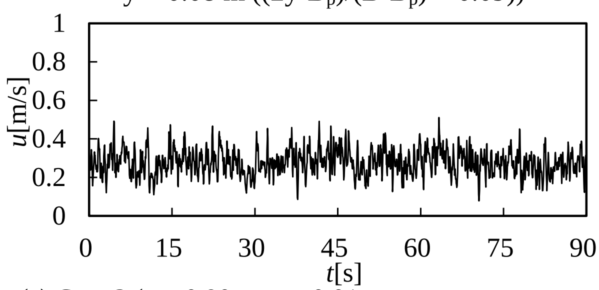

(e) Case 3 (x = 0.90 m, z = 0.01 m, y = 0.09 m ((2y-B_p)/(B-B_p) = 0.11))

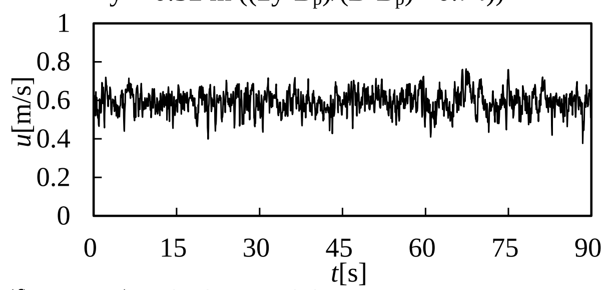

(f) Case 3 (x = 0.90m, z = 0.02 m, y = 0.35 m ((2y-B_p)/(B-B_p) = 0.86))

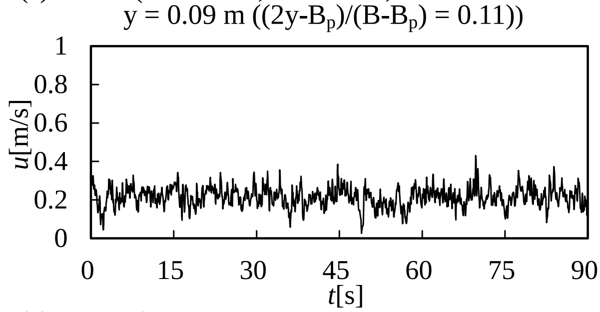

(g) Case 4 (x = 0.90 m, z = 0.01 m, y = 0.09 m ((2y-B_p)/(B-B_p) = 0.11))

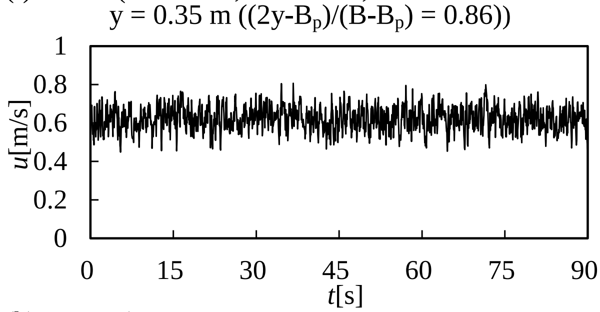

(h) Case 4 (x = 0.90m, z = 0.01 m, y = 0.32 m ((2y-B_p)/(B-B_p) = 0.77))

Figure 9. Times series variation of the flow velocity in *x* component

4. Conclusion

Experimental investigations were carried out using the consecutively assembled boulders as a countermeasure against gravel bed scouring around pier, under the rectangle and trapezoidal elliptical shape piers. The trapezoidal elliptical shape pier was proposed as a countermeasure to reduce deposition of driftwoods. Experimental investigations were also carried out on the conventional protection blocks as a comparative study. The findings of this study are as follows:

a) The undulation of the flow and water surface near the side wall was limited by installing a trapezoidal elliptical shape pier, and the effect of the unevenness of the water surface on the sidewall downstream of the pier could be reduced.

b) The conventional pier of the long rectangle elliptical shape is more prone to driftwood deposition because the front surface of the pier is vertical and the flow direction does not change in the direction of water depth except around the bottom surface. On the other hand, in the case of a trapezoidal elliptical shape pier, the impingement position differs in the vertical direction, and the approaching flow is dispersed, resulting in an unstable condition for driftwood and making it difficult for driftwood to be deposited.

c) The velocity measurement of the downstream component and the shape of the gravel bed revealed that no scouring was observed downstream of the installation of the assembled boulders even after a long experimental period (more 30 hours).

d) The time-averaged velocity of the downstream component near the gravel bed did not decay and its time-series change in the downstream direction was large at the downstream end of the piers in the case of the long rectangle elliptical shape, which is the conventional pier shape. The velocity near the gravel bed near the sidewall at the downstream end can be reduced by installing the assembled boulders in areas where the water surface is uneven due to the impact of the pier. The installation of the trapezoidal elliptical shape pier reduced the velocity near the gravel bed at the downstream end of the pier.

In summary, the trapezoidal elliptical shape pier of the piers is effective in reducing driftwood trapping and preventing riverbank erosion. Further, the installation of the consecutively assembled boulders on both sides of the piers was shown to be effective in preventing scouring of the riverbed.

References

Chiew, Y. M. (2002). Failure mechanisms of riprap layer around bridge piers. *Proceedings First International Conference on Scour of Foundations, ICSF-1,* Texas A&M University, College Station, Texas, USA November 17-20, pp.70-91.

Chiew, Y. M., & Lu, Y. (2005). Suction effects on riprap protection around bridge piers. *Proceedings of the 31st IHAR World Congress*, September11-16, pp. 1614-1620.

Ettema, R., Kirkil, G., & Muste, M. (2006). Similitude of largescale turbulence in experiments on local scour at cylinders. *Journal of Hydraulic Engineering*, *132*(1), 33-40. https://doi.org/10.1061/(ASCE)0733-9429(2006)132:1(33)

Furlan, P., Pfister, M., Matos, J., & Schleiss, A. J. (2018). Influence of density of large stems on the blocking probability at spillways. *7th International Symposium on Hydraulic Structures*, *Aachen. Germany*, pp. 15-18.

Japan Rivers Association. (2005). *Revised Explanation, River management facility structure order*. National Institute for Land and Infrastructure Development (ed.), Revised 20th Edition, Gihodo Shuppan.

Maeno, S., Yoshida, K., & Tanaka, R. (2014). Evaluation of hydrodynamic forces acting on bridge under flood in steep medium and small scale rivers. *Journal of JSCE Proceedings B1 (Hydraulic Engineering) (in Japanese)*, *54*, 883-888. https://doi.org/10.2208/jscejhe.70.I_883

Okamoto, T., Takebayashi, H., Suzuki, R., Sanjou, M., & Toda, K. (2017). Experimental study on porosity of driftwood blocking at a bridge and flood discharge of detour flow. *Japan Society for Natural Disaster Science (in Japanese)*, *36*(4), 447-461.

Takashi, I., Kurakami, Y., Sanagawa, T., & Nihei, Y. (2021). Experimental study on reduction of local scour due to various scour protection around Pier. *Journal of JSCE Proceedings B1 (Hydraulic Engineering) (in Japanese)*, *77*, 763-768. https://doi.org/10.2208/jscejhe.77.2_I_763

Umeda, S., Yamazaki, T., & Yuhi, M. (2010). Effects of foundation location on scour process around a cylindrical bridge pier. *Journal of JSCE Proceedings B1 (Hydraulic Engineering) (in Japanese)*, *54*, 835-840.

Vijayasree, B. A., Eldho, T. I., Mazumder, B. S., & Ahmad, N. (2019). Influence of bridge pier shape on flow field and scour geometry. *International Journal of River Basin Management*, *17*(1), 109-129. https://doi.org/10.1080/15715124.2017.1394315

Watanabe, G., Akamatsu, Y., Irie, T., & Ono, Y. (2015). The evaluation of dynamic water pressure to existing bridge pier in a river at a flood. *Journal of JSCE Proceedings A2 (Applied Mechanics) (in Japanese)*, *71*(2), I_359-I_368. https://doi.org/10.2208/jscejam.71.I_359

Yasuda, Y., & Fuchino, N. (2022). Assembled Boulder Installations in Improving Migration Routes for Aquatic Animals. *The Efficacy of Artificially River Basin Management - Under a Changing*, Intech Open, pp. 1-20. https://doi.org/10.5772/intechopen.105198

Zarrati, A. R., Gholami H., & Mashahir, M. B. (2004) Application of collar to control scouring around rectangular bridge piers. *Journal of Hydraulic Research*, *42*(1), 97-103. https://doi.org/10.1080/00221686.2004.9641188

Zhang, Z. (2022). Study on local scour protection countermeasures of bridge pier. *Highlights in Science, Engineering and Technology, AGECT, 28,* 464-470. https://doi.org/10.54097/hset.v28i.4878